A Simple, Effective Lead-Acid Battery Modeling Process for Electrical System Component Selection

Author(s): Robyn A. Jackey

Source: *SAE Transactions*, 2007, Vol. 116, SECTION 7: JOURNAL OF PASSENGER CARS: ELECTRONIC AND ELECTRICAL SYSTEMS (2007), pp. 219-227

Published by: SAE International

Stable URL: https://www.jstor.org/stable/44719887

2007-01-0778

A Simple, Effective Lead-Acid Battery Modeling Process for Electrical System Component Selection

Robyn A. Jackey
The MathWorks, Inc.

ABSTRACT

Electrical system capacity determination for conventional vehicles can be expensive due to repetitive empirical vehicle-level testing. Electrical system modeling and simulation have been proposed to reduce the amount of physical testing necessary for component selection [1, 2].

To add value to electrical system component selection, the electrical system simulation models must regard the electrical system as a whole [1]. Electrical system simulations are heavily dependent on the battery sub-model, which is the most complex component to simulate. Methods for modeling the battery are typically unclear, difficult, time consuming, and expensive.

A simple, fast, and effective equivalent circuit model structure for lead-acid batteries was implemented to facilitate the battery model part of the system model. The equivalent circuit model has been described in detail. Additionally, tools and processes for estimating the battery parameters from laboratory data were implemented. After estimating parameters from laboratory data, the parameterized battery model was used for electrical system simulation. The battery model was capable of providing accurate simulation results and very fast simulation speed.

INTRODUCTION

Modeling and simulation are important for electrical system capacity determination and optimum component selection. The battery sub-model is a very important part of an electrical system simulation, and the battery model needs to be high-fidelity to achieve meaningful simulation results. Current lead-acid battery models can be expensive, difficult to parameterize, and time consuming to set up. In this paper, an alternative lead-acid battery system model has been proposed, which provided drive cycle simulation accuracy of battery voltage within 3.2%, and simulation speed of up to 10,000 times real-time on a typical PC.

In Figure 1, a conventional design process is contrasted with Model-Based Design for electrical system component selection. The conventional design process for component selection, shown in Figure 1a, involves a costly, time-consuming, iterative process of building a test vehicle, evaluating performance, and then modifying the electrical system components. Using Model-Based Design, Figure 1b, introduces additional steps that make the overall design process more efficient. Model-Based Design requires only one or two iterations of modifying the test vehicle and re-verifying the electrical system design.

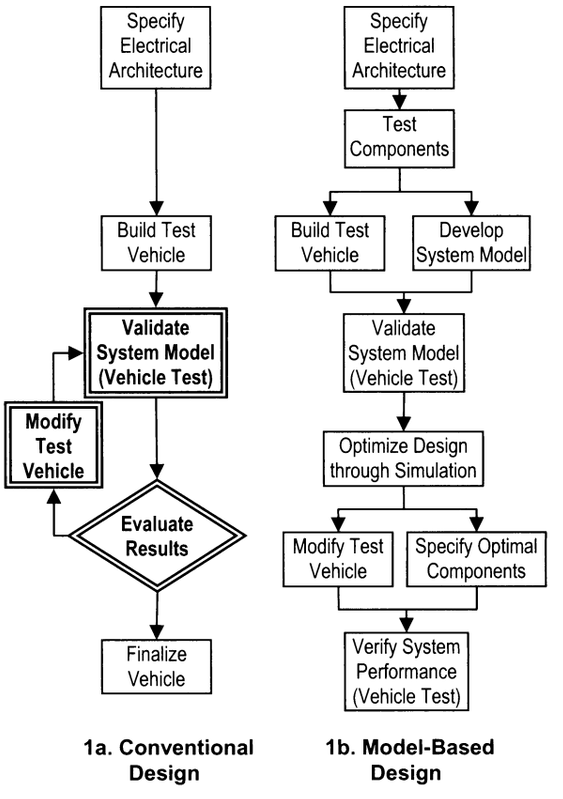

Figure 1 [6]: Component Selection Processes

A parameterization method has also been proposed, with testing requirements of standard discharge and charge curves. The battery model was used in electrical system simulations to study component sizing and selection for application to various vehicle electrical system configurations. The actual data collected during the battery modeling study were customer proprietary, and therefore were not included in this paper.

BATTERY MODEL

BATTERY MODEL STRUCTURE

A physical system lead-acid battery model was created[1]. The battery model was designed to accept inputs for current and ambient temperature, as shown in Figure 2. The outputs were voltage, SOC, and electrolyte temperature.

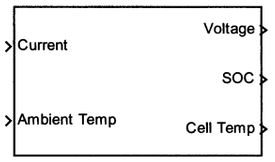

Figure 2 [6]: Battery Model

A diagram of the overall battery model structure is shown in Figure 3, which contains three major parts: a thermal model, a charge and capacity model, and an equivalent circuit model. The thermal model tracks electrolyte temperature and depends on thermal properties and losses in the battery. The charge and capacity model tracks the battery's state of charge (SOC), depth of charge remaining with respect to discharge current (DOC), and the battery's capacity. The charge and capacity model depends on temperature and discharge current. The battery circuit equations model simulates a battery equivalent circuit. The equivalent circuit depends on battery current and several nonlinear circuit elements.

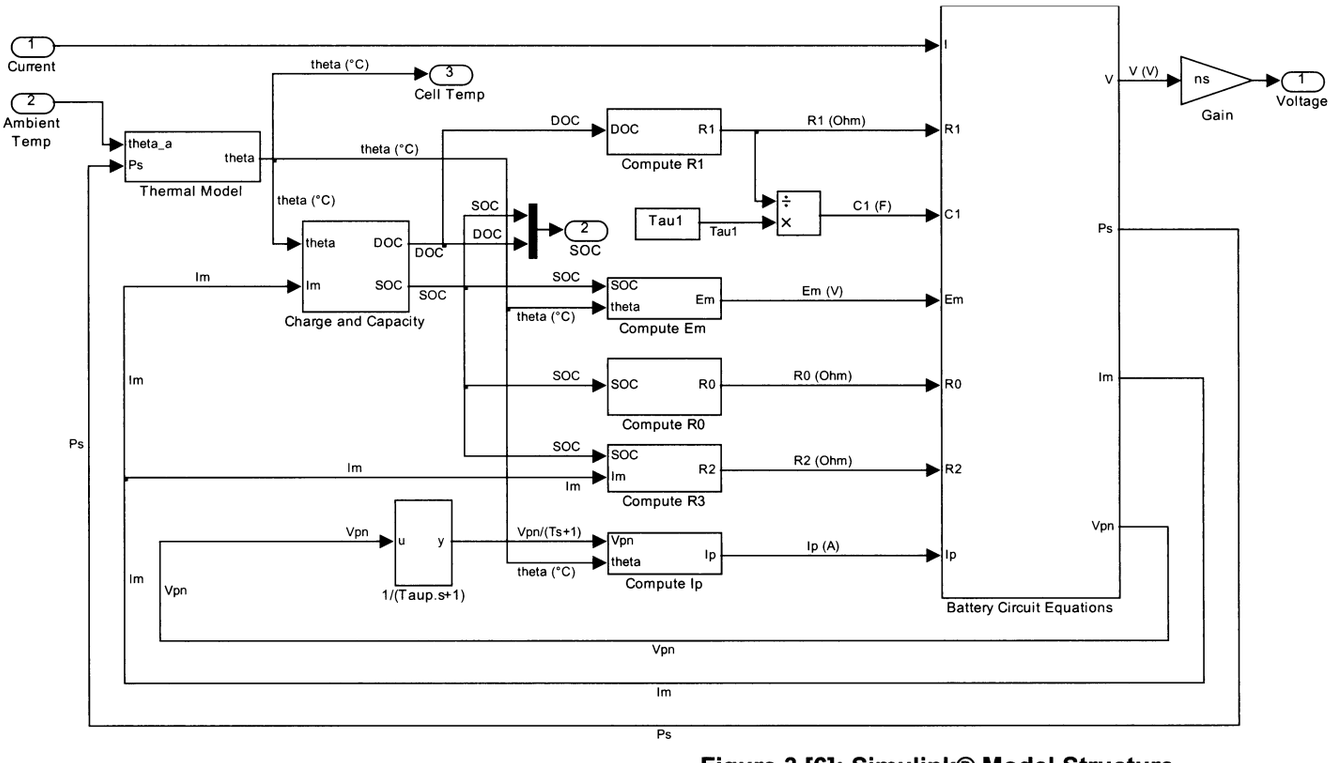

Figure 3 [6]: Simulink® Model Structure

[1] Modeled Using Simulink®

EQUIVALENT CIRCUIT

The structure of the battery circuit equations in Figure 3 was a simple nonlinear equivalent circuit [4], which is shown in Figure 4. The structure did not model the internal chemistry of the lead-acid battery directly; the equivalent circuit empirically approximated the behavior seen at the battery terminals. The structure consisted of two main parts: a main branch which approximated the battery dynamics under most conditions, and a parasitic branch which accounted for the battery behavior at the end of a charge.

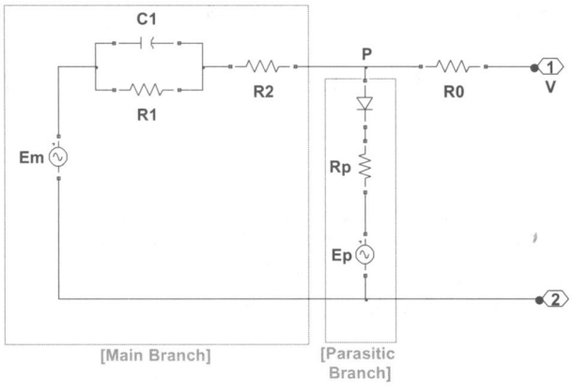

Figure 4 [6]: Battery Equivalent Circuit

The battery equivalent circuit represented one cell of the battery. The output voltage was multiplied by six, the number of series cells, to model a 12 volt automotive battery. In Figure 3, the number of series cells was entered into the Gain block with parameter value "ns." The voltage multiplication by six assumed that each cell behaved identically. Figure 4 shows the electrical circuit diagram containing elements that were used to create the battery circuit equations.

Each equivalent circuit element was based on nonlinear equations. The nonlinear equations included parameters and states. The parameters of the equations were dependent on empirically determined constants. The states included electrolyte temperature, stored charge, and circuit node voltages and currents. The equations were as follows:

Main Branch Voltage

Equation 1 approximated the internal electro-motive force (emf), or open-circuit voltage of one cell. The computation was performed inside the "Compute Em" block in Figure 3. The emf value was assumed to be constant when the battery was fully charged. The emf varied with temperature and state of charge (SOC).

$$E_m = E_{m0} - K_E(273+\theta)(1-SOC) \quad (1)$$

where:

E_m was the open-circuit voltage (EMF) in volts
E_{m0} was the open-circuit voltage at full charge in volts
K_E was a constant in volts / °C
θ was electrolyte temperature in °C
SOC was battery state of charge

Terminal Resistance

Equation 2 approximated a resistance seen at the battery terminals, and it was calculated inside the "Compute R0" block in Figure 3. The resistance was assumed constant at all temperatures, and varied with state of charge.

$$R_0 = R_{00}\left[1 + A_0(1-SOC)\right] \quad (2)$$

where:

R_0 was a resistance in Ohms
R_{00} was the value of R_0 at SOC=1 in Ohms
A_0 was a constant
SOC was battery state of charge

Main Branch Resistance 1

Equation 3 approximated a resistance in the main branch of the battery. The computation was performed inside the "Compute R1" block in Figure 3. The resistance varied with depth of charge, a measure of the battery's charge adjusted for the discharge current. The resistance increased exponentially as the battery became exhausted during a discharge.

$$R_1 = -R_{10}\ln(DOC) \quad (3)$$

where:

R_1 was a main branch resistance in Ohms
R_{10} was a constant in Ohms
DOC was battery depth of charge

Main Branch Capacitance 1

Equation 4 approximated a capacitance (or time delay) in the main branch. The computation was performed inside the "Compute C1" block in Figure 3. The time constant modeled a voltage delay when battery current changed.

$$C_1 = \tau_1 / R_1 \quad (4)$$

where:

C_1 was a main branch capacitance in Farads
τ_1 was a main branch time constant in seconds
R_1 was a main branch resistance in Ohms

Main Branch Resistance 2

Equation 5 approximated a main branch resistance. The computation was performed inside the "Compute R2" block in Figure 3. The resistance increased exponentially as the battery state of charge increased. The resistance also varied with the current flowing through the main branch. The resistance primarily affected the battery during charging. The resistance became relatively insignificant for discharge currents.

$$R_2 = R_{20}\frac{\exp\left[A_{21}(1-SOC)\right]}{1+\exp\left(A_{22}\, I_m / I*\right)} \tag{5}$$

where:

R_2 was a main branch resistance in Ohms
R_{20} was a constant in Ohms
A_{21} was a constant
A_{22} was a constant
E_m was the open-circuit voltage (EMF) in volts
SOC was battery state of charge
I_m was the main branch current in Amps
I was the a nominal battery current in Amps*

Parasitic Branch Current

Equation 6 approximated the parasitic loss current which occurred when the battery was being charged. The computation was performed inside the "Compute Ip" block in Figure 3. The current was dependent on the electrolyte temperature and the voltage at the parasitic branch. The current was very small under most conditions, except during charge at high SOC. Note that while the constant G_{po} was measured in units of seconds, the magnitude of G_{po} was very small, on the order of 10^{-12} seconds.

$$I_p = V_{PN} G_{p0} \exp\left(\frac{V_{PN}/\left(\tau_p s+1\right)}{V_{P0}} + A_p\left(1-\frac{\theta}{\theta_f}\right)\right) \tag{6}$$

where:

I_p was the current loss in the parasitic branch
V_{PN} was the voltage at the parasitic branch
G_{p0} was a constant in seconds
τ_p was a parasitic branch time constant in seconds
V_{P0} was a constant in volts
A_p was a constant
θ was electrolyte temperature in °C
θ_f was electrolyte freezing temperature in °C

CHARGE AND CAPACITY

The "Charge and Capacity" block in Figure 3 tracked the battery's capacity, state of charge, and depth of charge. Capacity measured the maximum amount of charge that the battery could hold. State of charge (SOC) measured the ratio of the battery's available charge to its full capacity. Depth-of-charge (DOC) measured the fraction of the battery's charge to usable capacity, because usable capacity deceased with increasing discharge current. The equations that tracked capacity, SOC, and DOC were as follows:

Extracted Charge

Equation 7 tracked the amount of charge extracted from the battery. The charge extracted from the battery was a simple integration of the current flowing into or out of the main branch. The initial value of extracted charge was necessary for simulation purposes.

$$Q_e(t) = Q_{e\_init} + \int_0^t -I_m(\tau)\,d\tau \tag{7}$$

where:

Q_e was the extracted charge in Amp-seconds
Q_{e_init} was the initial extracted charge in Amp-seconds
I_m was the main branch current in Amps
τ was an integration time variable
t was the simulation time in seconds

Total Capacity

Equation 8 approximated the capacity of the battery based on discharge current and electrolyte temperature. However, the capacity dependence on current was only for discharge. During charge, the discharge current was set equal to zero in Equation 8 for the purposes of calculating total capacity.

Automotive batteries were tested throughout a large ambient temperature range. Lab data across the entire tested current range showed that battery capacity began to diminish at temperatures above approximately 60°C. The look-up table (LUT) variable K_t in Equation 8 was used to empirically model the temperature dependence of battery capacity.

$$C(I,\theta) = \frac{K_c C_{o*} K_t}{1+(K_c-1)(I/I*)^{\delta}}, K_t = LUT(\theta) \tag{8}$$

where:

K_c was a constant
C_0 was the no-load capacity at 0°C in Amp-seconds*
K_t was a temperature dependent look-up table
θ was electrolyte temperature in °C
I was the discharge current in Amps
I was the a nominal battery current in Amps*
δ was a constant

State of Charge and Depth of Charge

Equation 9 calculated the SOC and DOC as a fraction of available charge to the battery's total capacity. State of charge measured the fraction of charge remaining in the battery. Depth of charge measured the fraction of usable charge remaining, given the average discharge current. Larger discharge currents caused the battery's charge to expire more prematurely, thus DOC was always less than or equal to SOC.

$$SOC = 1 - \frac{Q_e}{C(0,\theta)} \quad , \quad DOC = 1 - \frac{Q_e}{C(I_{avg},\theta)} \tag{9}$$

where:

SOC was battery state of charge
DOC was battery depth of charge
Q_e was the battery's charge in Amp-seconds
C was the battery's capacity in Amp-seconds
θ was electrolyte temperature in °C
I_{avg} was the mean discharge current in Amps

Estimate of Average Current

The average battery current was estimated as follows in Equation 10.

$$I_{avg} = \frac{I_m}{(\tau_1 s + 1)} \tag{10}$$

where:

I_{avg} was the mean discharge current in Amps
I_m was the main branch current in Amps
τ_1 was a main branch time constant in seconds

THERMAL MODEL

Electrolyte Temperature

The "Thermal Model" block in Figure 3 tracked the battery's electrolyte temperature. Equation 11 was modeled to estimate the change in electrolyte temperature, due to internal resistive losses and due to ambient temperature. The thermal model consists of a first order differential equation, with parameters for thermal resistance and capacitance.

$$\theta(t) = \theta_{init} + \int_0^t \frac{\left(P_s - \frac{(\theta - \theta_a)}{R_\theta}\right)}{C_\theta} d\tau \tag{11}$$

where:

θ was the battery's temperature in °C
θ_a was the ambient temperature in °C
θ_{init} was the battery's initial temperature in °C, assumed to be equal to the surrounding ambient temperature
P_s was the I^2R power loss of R_0 and R_2 in Watts
R_θ was the thermal resistance in °C / Watts
C_θ was the thermal capacitance in Joules / °C
τ was an integration time variable
t was the simulation time in seconds

BATTERY PARAMETER IDENTIFICATION

Parameterization of a battery model, such as the procedure proposed in [1], can be complex and difficult. The parameterization process in [1] requires difficult, nonstandard test procedures. A more automated approach was studied in detail and implemented. The automated approach used an optimization routine to adjust the battery model parameters, using discharge and charge test data.

DATA REQUIREMENTS

The parameterization method required standard lab test data. For discharge, full batteries were discharged at constant currents and temperatures. For charge, batteries were charged at constant current, until the terminal voltage approached the gassing voltage [5] for the battery. Then, the charges were continued at constant voltage, until the batteries reached a full charge. Several typical currents and ambient temperatures were used for the testing procedure. The quality and consistency of the lab data were very important in achieving a good fit with the lab data. The data showed some significant variability between tests, but the majority of the variability observed was at open circuit (no current). An example is shown in Figure 5.

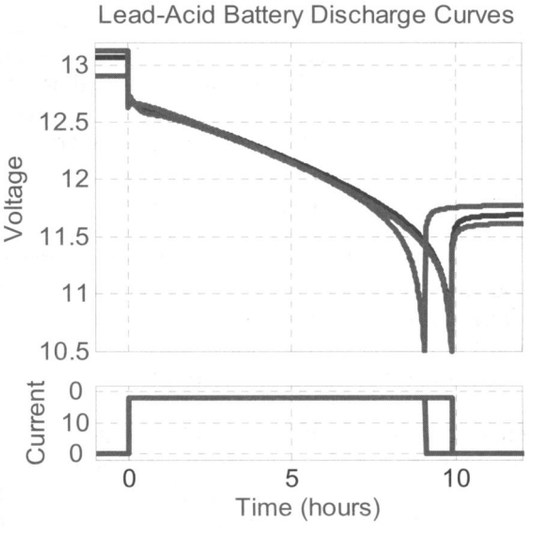

Figure 5 [6]: Variability of Measured Discharge Curves

AUTOMATIC PARAMETER TUNING

Due to the variability observed in battery discharge curves, a set of "average" discharge curves was used for the parameter tuning process. The average curves were created by calculating the mean voltage of all discharge tests taken at a unique combination of operating conditions (test runs at the same temperature and discharge current). An example is shown in Figure 6.

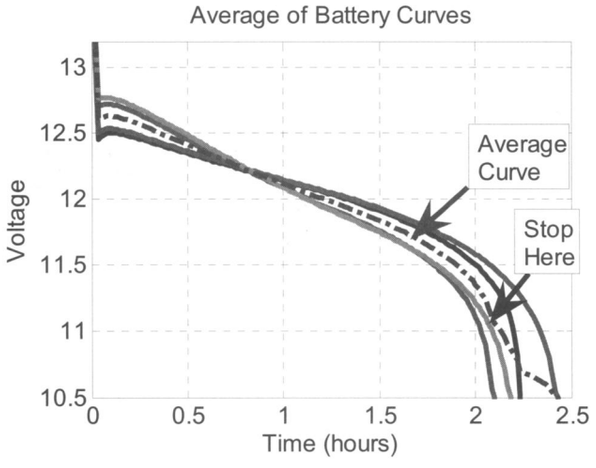

Figure 6 [6]: Mean-Value Discharge Curves

The overall estimation process involved several steps:

1. Optimizing capacity model
2. Optimizing discharge parameters
3. Optimizing charge and discharge parameters

Step 1: Capacity Model Optimization

The capacity was calculated from discharge test data for each tested temperature and discharge current. The mean-value discharge curves were used. Then, an optimization routine[2] was used to adjust the nonlinear capacity parameters to best fit the capacity equations to the measured mean capacities. These optimized parameter values were the final capacity parameters.

Step 2: Discharge Optimization

Next, the battery parameters were optimized to minimize the error between measured and simulated discharge curves. Only parameters that affected the discharge simulation were tuned[3]. The tuned parameters were given an initial value and min/max constraints.

The selection of the parameters and constraints for optimization was not a trivial process. Determining which parameters affected only the discharge cycles was not immediately straightforward. The parameter selections were the result of a significant amount of trial and error testing. Only parameters that were well exercised in the discharge curve data could be optimized, because of the risk of throwing off parameters which were dominant under other battery conditions, such as charging.

The optimization routine also adjusted the initial SOC of each discharge simulation, within reasonable constraints. By changing initial SOC, the entire simulated discharge curve effectively shifted down and to the left, or up and to the right as shown in Figure 7. Shifting the initial SOC allowed the simulated discharge curve to better align with the test data. Initial SOC was a necessary degree of freedom, because the batteries were not consistently fully charged before the test began.

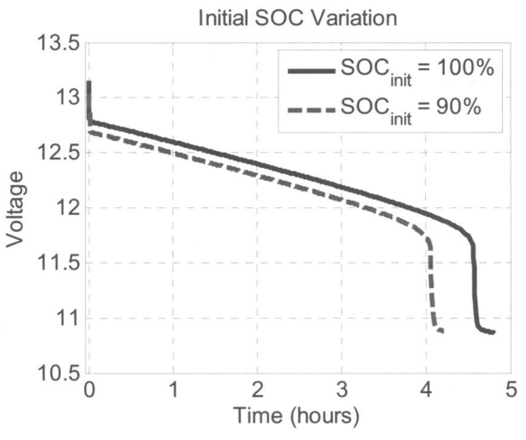

Figure 7 [6]: Initial SOC Variation

The last 25% of the measured discharge data was ignored for the initial optimization. The data was ignored because a large voltage error would occur if there was a slight error in the capacity, causing the simulated battery to fully discharge and the voltage to drop off before the tested battery voltage did. The voltage error would throw off the optimized parameters significantly.

After the optimization, each of the results was plotted for analysis. The curve fitting was considered to be reasonable. Some typical fitting variability under different battery conditions is shown in Figure 8 and Figure 9. Some variability was typical at the beginning and end of the discharge cycle, including differences in the battery's capacity. Some of the differences were attributed to using different physical batteries for each lab test.

[2] Using Optimization Toolbox®
[3] Using Simulink Parameter Estimation®

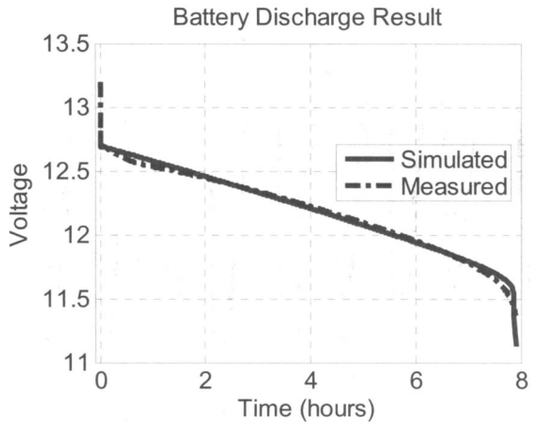

Figure 8 [6]: Discharge Curve Example 1

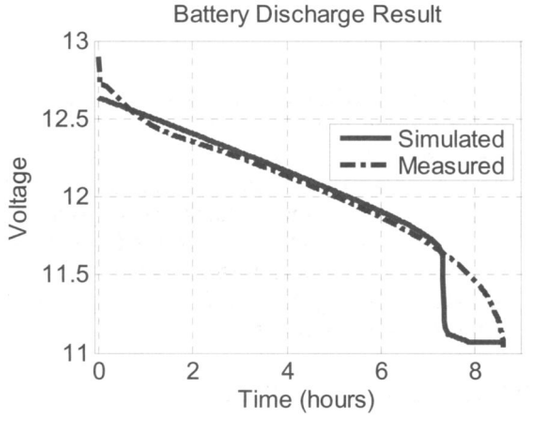

Figure 9 [6]: Discharge Curve Example 2

Step 3: Combined Charge and Discharge Optimization

After the battery discharge parameters were fully optimized, then the charge curves were optimized. However, while some parameters primarily affected the battery charging condition, other parameters affected both the discharge and charge. Consequently, both discharge and charge test data and parameters were used in the final optimization. Simulated voltage and current both needed to be optimized for charging curves only, because neither was held constant throughout the entire tests. Weight coefficients were used to balance the optimization of the current vs. voltage errors, because the raw current and voltage values had some magnitude difference.

The results were reasonable with respect to the battery test data. Many of the simulated and measured results lined up very closely. Note that the discharge test results did worsen slightly during the combined charge and discharge optimization (step 3), but the curves were still very close. Some of the worst-case results observed are shown in Figure 10 and Figure 11.

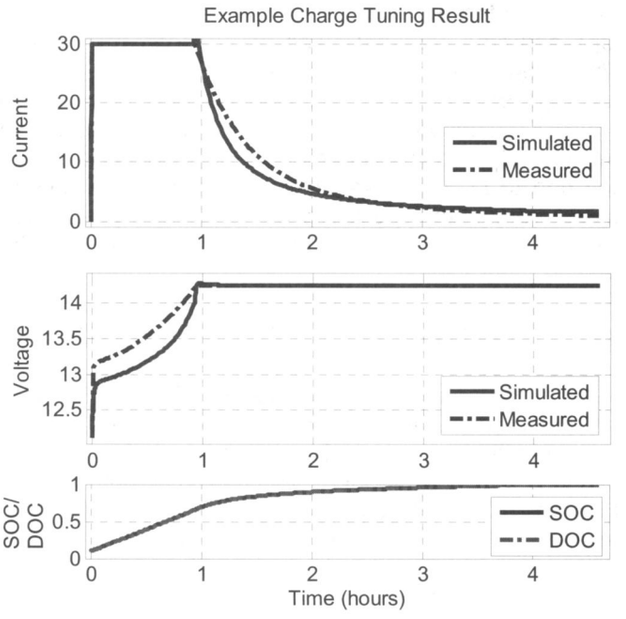

Figure 10 [6]: Final Charge Curve - Worst Case Example Observed

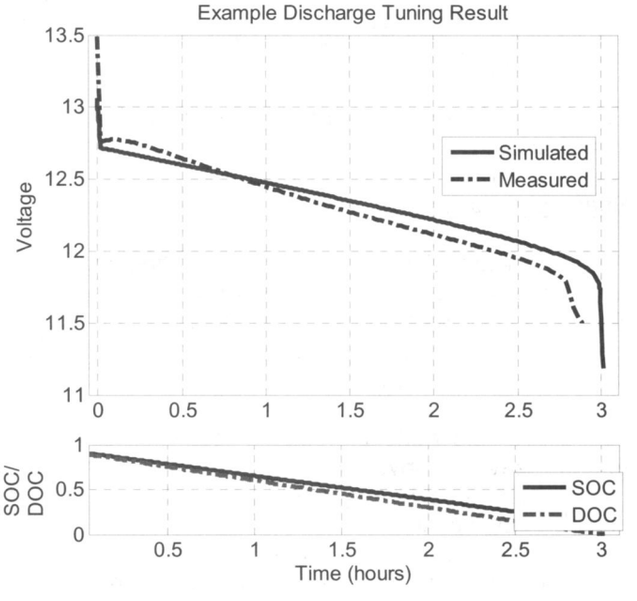

Figure 11 [6]: Final Discharge Curve - Worst Case Example Observed

Additional Tuning

After the major optimizations, the battery's thermal model was adjusted manually. The thermal resistance and capacitance were adjusted based on data from the application of the battery in a vehicle test. The adjustment was made because the thermal properties depend heavily on the installation of the battery in a vehicle.

The parameters R_1 and τ_1 affected the end of discharge slope and time constant. The parameters were tuned[4] with a few discharge curves that included the after-discharge settling time, similar to the curves shown in **Figure 5**. The parameters were not well-exercised in the rest of the battery parameter estimation process, so they had to be tuned separately. Once the parameter values were determined, the entire fitting process was re-run with the new values to ensure an optimal fit to the lab data.

USE IN ELECTRICAL SYSTEM SIMULATIONS

The final battery model block, shown in Figure 12, was used within an electrical system simulation model. Multiple battery sizes were parameterized to facilitate electrical system component selection. The battery block was used in drive cycle simulations with different parameters for the different battery sizes.

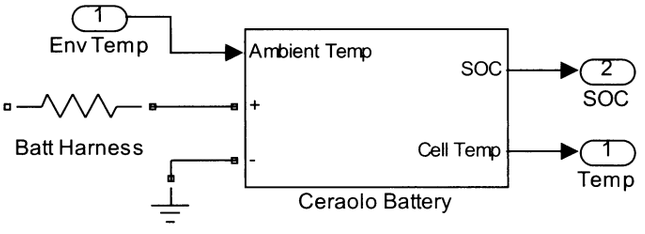

Figure 12 [6]: Battery Model for Electrical System Simulation

Speed and Accuracy

The battery model was capable of simulating one hour of simulation time in less than half a second of real time. The simulation was performed on a typical PC using a Runge-Kutta (4, 5) variable step solver. Open-loop input current data was used at a 1 second sample time.

To validate the battery model, a test vehicle was run through several drive cycles to gather actual RPM, temperature, and battery current and voltage data to compare to the simulation. An example is shown in Figure 13. The battery model was simulated using RPM, temperature, and current inputs. On a 1-hour stop-and-go cycle, the accuracy of the simulated battery model voltage was within 3.2% (0.42 Volts) throughout. On a 1-hour idling simulation with transmission in park, the voltage was within 1.2% (0.15 Volts).

[4] Using Simulink Parameter Estimation®

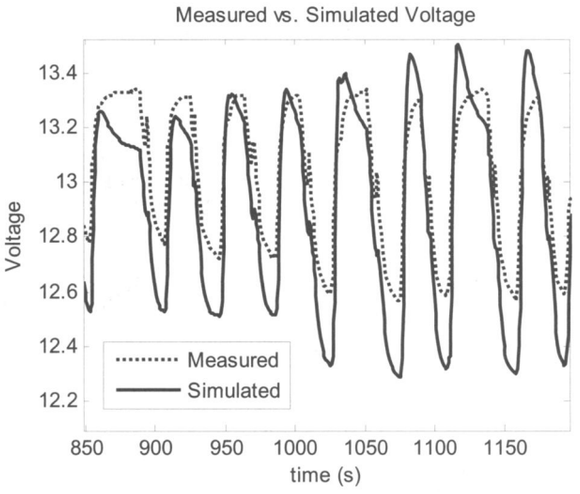

Figure 13 [6]: Battery Simulation Voltage

FUTURE WORK

Battery modeling is a difficult and time-consuming task. Given additional time, many additions and changes could have been made to improve the results. Improvements have a point of diminishing returns when the error experienced in the battery model becomes smaller than the variability experienced with real batteries. However, there were a few improvements that could have been investigated to further improve the battery parameterization process.

Battery Aging and Typical Performance

Undesired aging effects can occur when test batteries are fully charged and discharged repeatedly. In this paper, a new battery was tested for only four discharge and charge cycles, to minimize aging effects. However, the possibility of instead obtaining parameterization data with weaker, broken-in batteries should be studied. Using slightly aged batteries might improve the battery parameterization, allowing simulation of more typical electrical system performance.

Simpler Application to Other Batteries

Approximating parameters for a battery of the same chemistry but different capacity should be possible without repeating the entire data collection and optimization process. In this paper, two battery capacities were parameterized, however, a direct relationship could not be found between the optimized parameters of each of the two batteries. The lack of a direct relationship between parameters of two batteries having the same chemistry but different capacity could have been caused by "noise" in the battery data or by some parameters not being sensitive. The parameter relationship for different capacities would be a very useful topic for further study, because a capacity relationship could provide a cost savings if a few known adjustments could be made to the parameters to create

additional battery sizes without repeating the entire test process for each new battery capacity.

Measuring Battery Capacity

Battery capacity was very difficult to estimate correctly. One reason for the difficulty was battery variability. Another reason for the difficulty was that ensuring the battery was fully charged before discharge testing was not easy. Fully charging the battery was more of an issue at higher temperatures where charging losses are significant, and thus achieving a full charge becomes difficult. The charging difficulties at higher temperatures should be taken into consideration during the lab testing process. The batteries should be as completely charged as possible before discharge tests begin.

CONCLUSION

A lead-acid battery model was developed, along with tools to parameterize the model from laboratory data. Construction of an equivalent circuit model has been described. A semi-automated process was used to estimate parameters for the battery model from laboratory data. The completed battery model simulated at approximately 10,000 times real-time. The accuracy of the simulated battery model voltage was within 3.2% in comparison to vehicle drive cycle measurements.

ACKNOWLEDGEMENTS

Special thanks to Andrew Bennett of The MathWorks for providing the original battery model structure and for supporting the model development. Thanks also to Bora Eryilmaz of The MathWorks for supporting the battery parameterization with Simulink Parameter Estimation, and to Peter Maloney of The MathWorks for modeling support and for reviewing this technical paper. Also, data and application feedback provided by Nick Chung and JK Min of Hyundai Motor Company were instrumental in the project's success.

REFERENCES

1. Schöttle, R., W. Müller, H. Meyer, and E. Schoch. "Methods for the Efficient Development and Optimization of Automotive Electrical Systems," 970301, SAE, Warrendale, PA, 1997.
2. Wootaik Lee, Hyunjin Park, Myoungho Sunwoo, Byoungsoo Kim, Dongho Kim. "Development of a Vehicle Electric Power Simulator for Optimizing the Electric Charging System," 2000-01-0451, SAE, Warrendale, PA, 2000.
3. Ceraolo, Massimo and Stefano Barsali. "Dynamical Models of Lead-Acid Batteries: Implementation Issues," *IEEE Transactions on Energy Conversion.* Vol. 17, No. 1, IEEE, March 2002.
4. Ceraolo,. "New Dynamical Models of Lead-Acid Batteries," *IEEE Transactions on Power Systems*. Vol. 15, No. 4, IEEE, November 2000.
5. D. Linden and T. B. Reddy (editors), Handbook of Batteries, 3rd edition, McGraw-Hill, New York, NY, 2001.
6.

CONTACT

Robyn A. Jackey
Technical Consultant, The MathWorks, Inc.
39555 Orchard Hill Place, Suite 280
Novi, MI 48375
Email: robyn.jackey@mathworks.com